Biosensors

DOI: 10.1002/anie.201001428

A Graphene Oxide Based Immuno-biosensor for Pathogen Detection**

*Jae Hwan Jung, Doo Sung Cheon, Fei Liu, Kang Bum Lee, and Tae Seok Seo**

The development of novel biosensors for highly sensitive, selective, and rapid pathogen detection is of paramount importance for medical diagnostics, food safety screening, and environmental pollution monitoring. Graphene oxide (GO), which is well known as a promising precursor for graphene, has great potential for use in biosensors because of its unique characteristics such as facile surface modification,[1] high mechanical strength,[2] good water dispersibility,[3] and photoluminescence.[4] Recently, Lu et al., and Liu et al. demonstrated the usefulness of the fluorescence quenching properties of GO in DNA biosensing.[5] Gold nanoparticles (AuNPs) have been shown to be excellent quenchers for organic fluorescent tags,[6] semiconductor nanocrystals,[7] and oxidized carbon nanotubes.[8] Herein, we demonstrate a GO-based immuno-biosensor for detecting a rotavirus as a pathogen model. The detection occurs with high sensitivity and selectivity by GO photoluminescence quenching induced by fluorescence resonance energy transfer (FRET) between GO sheets and AuNPs.

A GO-based immuno-biosensor system is shown in Figure 1. GO, which was synthesized by a modified Hummers method, was deposited on an amino-modified glass surface.[9] The disruption of the sp^2 structure of graphene crystals during the oxidation process results in the recombination of electron–hole pairs localized within small sp^2 carbon domains that are embedded in an sp^3 matrix, thus resulting in photoluminescence with a quantum yield of 70.3% relative to the fluorescein dye.[10] A homogenous solution of GO shows a broad fluorescence emission peak around 547 nm upon excitation at 400 nm (Figure S1a,b in the Supporting Information). Since the GO has negatively charged functional groups such as carboxylic acids, hydroxy groups, and epoxides,[11] the GO sheets are bound to the positive surface through an electrostatic interaction, which is strong enough to ensure that the GO sheets are retained during a washing step.

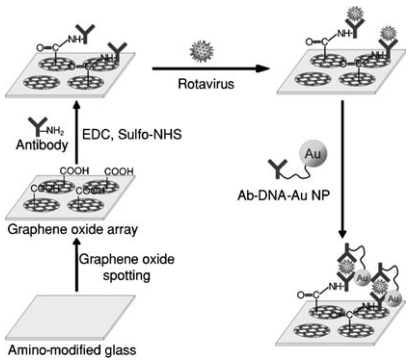

Figure 1. Illustration of a GO-based immuno-biosensor.

The antibodies for rotavirus are immobilized on the GO array by a carbodiimide-assisted amidation reaction, and the rotavirus cell is captured by specific antigen–antibody interaction (Figure 1). The capture of a target cell was verified by observing the fluorescence quenching of GO by FRET between the GO and AuNPs. To realize such a novel GO immuno-biosensor, we first synthesized AuNP-linked antibodies (Ab-DNA-AuNP complexes; Figure S2 in the Supporting Information) which were bridged with 100-mer single-stranded DNA molecules. The DNA molecule was used as a mediator as the synthetic method, which is based on phosphoramidite chemistry, provides facile control of distance between Ab and AuNPs, so the AuNPs are placed close to the GO surface. The high affinity of amino functional groups of the DNA nucleotides for multiple AuNPs leads to an enhancement of the quenching efficiency of GO.[12] When the Ab-DNA-AuNP complexes were selectively bound to the target cells that were attached to the GO arrays, a reduction in the fluorescence emission of GO by quenching was detected, thus enabling the identification of pathogenic target cells.

AFM analysis was performed to obtain the topographical profile for each step during the fabrication of GO immuno-biosensor (Figure 2). GO sheets ranging from 500 nm to 2 μm in lateral dimension (Figure S1b in the Supporting Information) were dispersed uniformly as mono- and bilayers, which were determined by measuring the height (1.1 nm) between the two black marks in Figure 2a. The antibody-linked GO array shows brighter spots, particularly at the edges, and also folded structures, which contain many carboxylic acid groups.[11] The measured height of 11.9 nm corresponds to the theoretical value of an antibody (10–15 nm) and approximately 15.3% area per spot was linked by antibodies.[13] Once the target rotavirus was captured, the height of the complexes increased to approximately 81 nm. Considering that the size

[*] J. H. Jung, F. Liu, Prof. T. S. Seo
Department of Chemical and Biomolecular Engineering
Korea Advanced Institute of Science and Technology (KAIST)
373-1, Guseong-dong, Yuseong-gu
Daejeon, 305-701 (Republic of Korea)
Fax: (+82) 42-350-3910
E-mail: seots@kaist.ac.kr
Dr. D. S. Cheon, K. B. Lee
Division of Enteric and Hepatitis Viruses
Korea Centers for Disease Control and Prevention (KCDC)
5, Nokbun-dong, Eunpyung-gu, Seoul, 122-701 (Republic of Korea)

[**] This work was supported by Korean Ministry of Environment as "The Eco-Technopia 21" project.

Supporting information for this article is available on the WWW under http://dx.doi.org/10.1002/anie.201001428.

WILEY InterScience DISCOVER SOMETHING GREAT
© 2010 Wiley-VCH Verlag GmbH & Co. KGaA, Weinheim

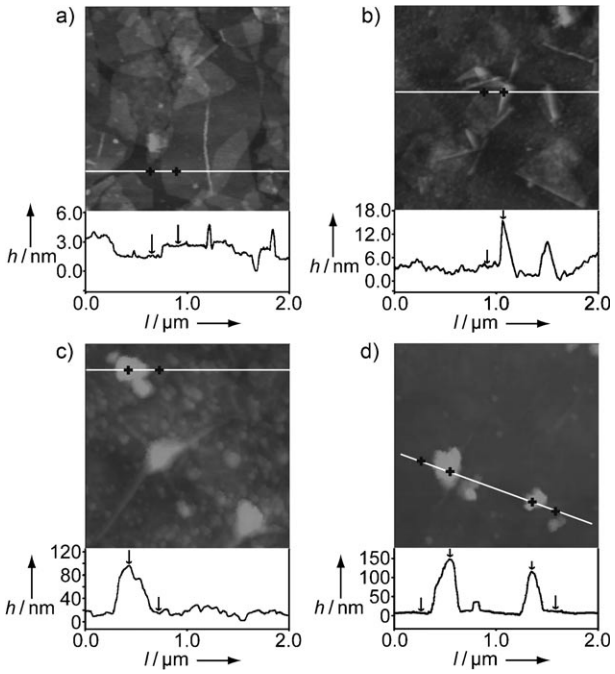

Figure 2. AFM images (top) and height profile (taken along the white line in the AFM images; bottom) of the GO based immunoassay: a) Pristine GO sheets; b) Ab-immobilized GO sheets; c) Ab–rotavirus linked GO sheets; and d) Ab-DNA-AuNP complexes linked to the target cells on the GO sheets.

of a rotavirus ranges from 70 to 100 nm, the height profile in Figure 2c confirms the specific cell capture on the GO array. When the Ab-DNA-AuNP complex was synthesized with an Ab/AuNP molar ratio of 150:30, the size of the Ab-DNA-AuNP conjugates ranged from 150 to 200 nm, which resulted from the aggregation of 15 nm AuNPs through the DNA molecules (Figure S3 in the Supporting Information). When the exposed antibodies of Ab-DNA-AuNPs were reacted with the target cells, the final complexes on the GO array had heights of approximately 142 nm and 103.7 nm (Figure 2d), thus confirming that the AuNPs are sufficiently close to the GO surface for FRET to occur. The fluorescence quenching efficiency of the GO array is affected by several factors such as the concentration of immobilized Ab, the area of the GO sheets, and the number of AuNP quenchers. Ideally, in order for maximum quenching to occur, a large number of AuNPs should interact with a very small area of GO sheets. To this end, three kinds of Ab-DNA-AuNP complexes were prepared by reacting Ab (600 pmol) with AuNP solutions with concentrations of 4 pmol, 40 pmol, or 120 pmol. As the AuNP concentration was increased to 120 pmol, more AuNPs were covalently bound to the amino group of bases in the DNA, thus resulting in an AuNP assembly with an average diameter of 180 nm. Use of a 4 pmol AuNP solution resulted in AuNP aggregates with an average diameter of 80 nm.

The quenching efficiencies of the three Ab-DNA-AuNP conjugates were compared with a negative control (NC) experiment in which the procedure shown in Figure 1 was followed except that the cell incubation step was omitted. The fluorescence intensities of quadruplicate spots were reduced as the molar ratio of Ab to AuNPs increased (Figure 3a), whereas the bright fluorescence emission signal is that of the pristine GO. The negatively charged GO surface and the immobilized Ab assisted in preventing any associated non-specific binding of Ab-DNA-AuNP complexes. When the

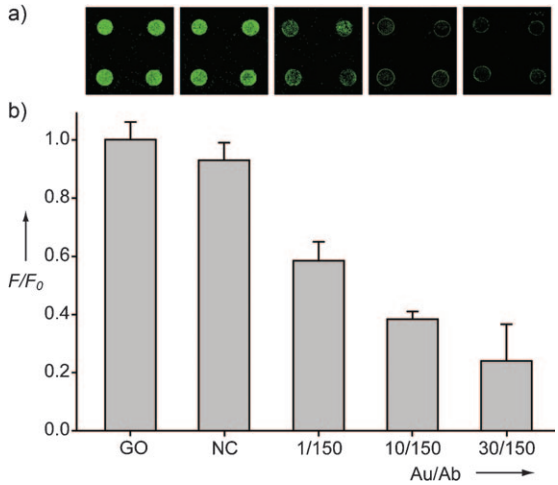

Figure 3. a) Fluorescence scanning images of a GO immunoarray depend on the number of AuNPs in the Ab-DNA-AuNP complexes, which were synthesized with AuNP/Ab molar ratios of 1:150, 10:150, and 30:150. b) Relative fluorescence emission intensity (F) compared to the fluorescence intensity of the pristine GO (F_0) when treated with three different Ab-DNA-AuNP complexes. The average quenching efficiencies were 0.41 for Au/Ab = 1:150, 0.61 for Au/Ab = 10:150, and 0.76 for Au/Ab = 30:150.

average fluorescence intensity of the pristine GO array was normalized to 1, the average quenching efficiencies of GO were calculated as 41%, 61%, and 76% with the Ab-DNA-AuNP complexes synthesized with an Ab/AuNP molar ratio of 150:1, 150:10, and 150:30, respectively (Figure 3b). Thus, the Ab-DNA-AuNPs that bear more AuNPs lead to drastic fluorescence reduction of GO, thus allowing a sensitive rotavirus detection.

We subsequently performed a limit-of-detection (LOD) study by varying the concentration of rotavirus from 10^3 pfu ml^{-1} to 10^5 pfu ml^{-1} (Figure 4; pfu = plaque-forming unit). As a quencher we employed the Ab-DNA-AuNP conjugate synthesized with a molar ratio of 150:30, which showed the highest quenching efficiency in Figure 3. The GO quenching effect was enhanced in proportion to the input cell number relative to the fluorescence intensity of the pristine GO array. Although the fluorescence difference is not significant between the negative control and the cell concentration of 10^3 pfu mL^{-1}, use of cell solutions with concentrations of 10^4 and 10^5 pfu mL^{-1} resulted in distinguishable fluorescence intensity reductions of 44 and 76%, respectively. The input cell concentration of 10^5 pfu mL^{-1} results in the maximized GO quenching efficiency of up to 85%. If we assume that the threshold of quenching efficiency should be more than 70% to recognize the target rotavirus, 10^5 pfu mL^{-1} is a LOD under our experimental conditions, and is com-

 © 2010 Wiley-VCH Verlag GmbH & Co. KGaA, Weinheim

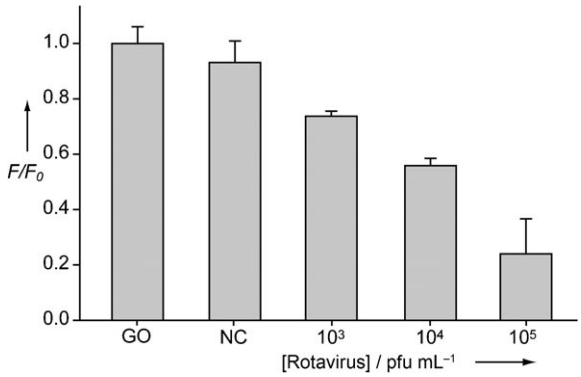

Figure 4. LOD study of the GO immunosensor for pathogen detection. The fluorescence quenching efficiency relative to the pristine GO was dependent on the input cell concentration, which ranged from 10^3 to 10^5 pfu mL^{-1}. The fluorescence quenching efficiency was 0.26 for 10^3 pfu mL^{-1}, 0.44 for 10^4 pfu mL^{-1}, and 0.76 for 10^5 pfu ml^{-1}.

parable to the LOD value of a conventional ELISA technology.[14]

To demonstrate the specificity for detecting pathogens on a GO immunoassay, we performed the cell incubation with poliovirus and variola virus following the same procedure as above (10^5 pfu mL^{-1} input cell concentration), and then compared the resulting fluorescence image with that of the rotavirus (Figure 5). Since the GO array was initially linked to the rotavirus-specific antibody, the unmatched poliovirus and variola virus did not cause the fluorescence quenching eventually by showing a similar level of fluorescence intensities to the negative control. In the case of the rotavirus, however, a quenching enhancement in excess of 15-fold was observed compared with other viruses. The significant difference of fluorescence intensities clearly suggests that the GO based immuno-biosensor can perform a specific pathogenic virus detection.

In conclusion, we have developed a novel GO-based immuno-biosensor for highly sensitive, selective, and rapid virus detection, and this platform can be expanded to a GO microarray format for multiple pathogen analysis. The unique fluorescence emission property and facile fabrication method of GO sheets from cheap graphite resources provide great potential of GO to be applied for biosensors as well as molecular diagnostics as a novel fluorescent tag.

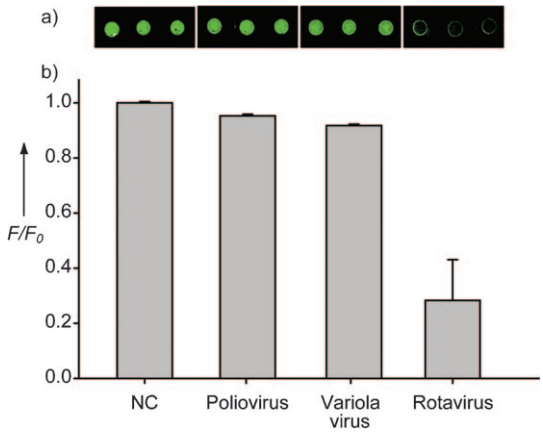

Figure 5. Specificity of the GO-based immuno-biosensor. While the GO array incubated with poliovirus and variola virus shows a bright fluorescence signal similar to the NC (a), the target rotavirus causes a fluorescence quenching effect that is 15 times higher by FRET from GO (b).

Experimental Section

GO sheets were synthesized by a modified Hummers method.[9] Rotavirus, poliovirus, and variola virus were kindly donated by Korea Centers for Disease Control and Prevention (KCDC). Rotavirus monoclonal antibodies were purchased from Fitzgerald Industries International. Oligonucleotides were synthesized by Bioneer, Korea, and Au nanoparticles were synthesized following the method reported by Grabar et al.[15] Amino-modified glass slides were purchased from Nuricell, Korea.

Immobilization of antibodies: 1 μL of GO solution (0.3 mg mL^{-1}) was deposited on the amino modified glass by electrostatic force and dried in a humid chamber. After washing with distilled water, 0.5 μL of 1-ethyl-3-[3-dimethylaminopropyl]carbodiimide (EDC; 0.5 mM) and *N*-hydroxysulfo-succinimide (sulfo-NHS; 1.0 mM) were added, and incubated for 30 min at 37 °C. A solution of rotavirus antibodies (1 μL, 1 μg mL^{-1}) was incubated on the same spot for 3 h to enable the covalent linkage on the GO surface.

Pathogen detection: Rotavirus solution (1 μL) was added to the antibody-immobilized GO array and bound by a specific antigen–antibody interaction. The rotavirus concentration ranged from 10^3 pfu mL^{-1} to 10^5 pfu mL^{-1}. After incubation for 1 h at 37 °C, 1 μL of an engineered Ab-DNA-AuNP conjugate (0.5 mg mL^{-1}) was added and incubated for 3 h to allow Ab-DNA-AuNP complexes to be linked to the captured target cell and place the AuNPs close to the GO surface. After gentle washing with distilled water, the fluorescence signal of the GO array was measured by a GenePix 4000 A scanner (Axon Instruments, Inc., US) with 532 nm excitation wavelength (PMT detector voltage = 800 V).

Characterization of the GO surface: AFM images of the modified GO array were obtained with a tapping mode at a 300 kHz scan rate and a 256 × 256 pixel resolution (Veeco Instruments Inc., USA), and analyzed by a Nanoscope (R) III software (Veeco Instruments Inc., USA).

Received: March 10, 2010
Published online: July 2, 2010

Keywords: biosensors · fluorescence · FRET · graphene · nanoparticles

[1] a) N. Mohanty, V. Berry, *Nano Lett.* **2008**, *8*, 4469–4476; b) M. Zhou, Y. Zhai, S. Dong, *Anal. Chem.* **2009**, *81*, 5603–5613; c) J.-F. Wu, M.-Q. Xu, G.-C. Zhao, *Electrochem. Commun.* **2010**, *12*, 175–177; d) X. Zuo, S. He, D. Li, C. Peng, Q. Huang, S. Song, C. Fan, *Langmuir* **2010**, *26*, 1936–1939; e) Z. Wang, X. Zhou, J. Zhang, F. Boey, H. Zhang, *J. Phys. Chem. C* **2009**, *113*, 14071–14075.

[2] D. A. Dikin, S. Stankovich, E. J. Zimney, R. D. Piner, G. H. B. Dommett, G. Evmenenko, S. T. Nguyen, R. S. Ruoff, *Nature* **2007**, *448*, 457–460.

[3] Z. Liu, J. T. Robinson, X. Sun, H. Dai, *J. Am. Chem. Soc.* **2008**, *130*, 10876–10877.

[4] X. Sun, Z. Liu, K. Welsher, J. T. Robinson, A. Goodwin, S. Zaric, H. Dai, *Nano Res.* **2008**, *1*, 203–212.

[5] a) C.-H. Lu, H.-H. Yang, C.-L. Zhu, X. Chen, G.-N. Chen, *Angew. Chem.* **2009**, *121*, 4879–4881; *Angew. Chem. Int. Ed.*

 © 2010 Wiley-VCH Verlag GmbH & Co. KGaA, Weinheim

2009, *48*, 4785 – 4787; b) F. Liu, T. S. Seo, *Biosens. Bioelectron.* **2010**, *25*, 2361 – 2365.
[6] B. Dubertret, M. Calame, A. J. Libchaber, *Nat. Biotechnol.* **2001**, *19*, 365 – 370.
[7] a) T. Pons, I. L. Medintz, K. E. Sapsford, S. Higashiya, A. F. Grimes, D. S. English, H. Mattoussi, *Nano Lett.* **2007**, *7*, 3157 – 3164; b) R. Gill, I. Willner, I. Shweky, U. Banin, *J. Phys. Chem. B* **2005**, *109*, 23715 – 23719.
[8] a) Y.-Y. Ou, M. H. Huang, *J. Phys. Chem. B* **2006**, *110*, 2031 – 2036; b) L. Liu, T. Wang, J. Li, Z.-X. Guo, L. Dai, D. Zhang, D. Zhu, *Chem. Phys. Lett.* **2003**, *367*, 747 – 752.
[9] a) W. S. Hummers, R. E. Offeman, *J. Am. Chem. Soc.* **1958**, *80*, 1339 – 1339; b) Y. Xu, Z. Liu, X. Zhang, Y. Wang, J. Tian, Y. Huang, Y. Ma, X. Zhang, Y. Chen, *Adv. Mater.* **2009**, *21*, 1275 – 1279.
[10] a) G. Eda, Y.-Y. Lin, C. Mattevi, H. Yamaguchi, H.-A. Chen, I-S. Chen, C.-W. Chen, M. Chhowalla, *Adv. Mater.* **2010**, *22*, 505 – 509; b) J. H. Brannon, D. Magde, *J. Phys. Chem.* **1978**, *82*, 705 – 709.
[11] S. Stankovich, D. A. Dikin, R. D. Piner, K. A. Kohlhaas, A. Kleinhammes, Y. Jia, Y. Wu, S. T. Nguyen, R. S. Ruoff, *Carbon* **2007**, *45*, 1558 – 1565.
[12] M. Cárdenas, J. Barauskas, K. Schillen, J. L. Brennan, M. Brust, T. Nylander, *Langmuir* **2006**, *22*, 3294 – 3299.
[13] a) K. Maehashi, T. Katsura, K. Kerman, Y. Takamura, K. Matsumoto, E. Tamiya, *Anal. Chem.* **2007**, *79*, 782 – 787; b) A. S. Paulo, R. Garcia, *Biophys. J.* **2000**, *78*, 1599 – 1605.
[14] S. S. R. Ajjampur, P. Rajendran, S. Ramani, I. Banerjee, B. Monica, P. Sankaran, V. Rosario, R. Arumugam, R. Sarkar, H. Ward, G. Kang, *J. Med. Microbiol.* **2008**, *57*, 1364 – 1368.
[15] K. C. Grabar, R. G. Freeman, M. B. Hommer, M. J. Natan, *Anal. Chem.* **1995**, *67*, 735 – 743.

 © 2010 Wiley-VCH Verlag GmbH & Co. KGaA, Weinheim